Journal of Catalysis **205,** 115–122 (2002)
doi:10.1006/jcat.2001.3427, available online at http://www.idealibrary.com on IDEAL®

Characterization of Surface Vanadia Forms on V/Ti–Oxide Catalyst via Temperature-Programmed Reduction in Hydrogen and Spectroscopic Methods

Dmitri A. Bulushev, Lioubov Kiwi-Minsker,[1] Fabio Rainone, and Albert Renken

Swiss Federal Institute of Technology, LGRC-EPFL, CH-1015 Lausanne, Switzerland

Received June 4, 2001; revised September 28, 2001; accepted October 1, 2001

Surface vanadia species formed on vanadia/titania catalysts consisting of 0.2–2.6 monolayers (ML) of VO_x have been characterized by FT–Raman spectroscopy under controlled atmosphere, temperature-programmed reduction in hydrogen (TPR), and solubility in diluted HNO_3. Three types of species were observed with the maximum peak temperatures as follows: isolated monomeric species ($\leq$770–780 K), polymeric species (810 K), and bulk amorphous V_2O_5 (852 K). During the reduction, the V=O bond of the monomeric species with tetracoordinated vanadium disappears as shown by diffuse reflectance infrared Fourier transform spectroscopy. A formation of new hydroxyl groups with a basic character was observed. The monomeric species was found to be chemically stable with respect to diluted HNO_3. Bulk amorphous V_2O_5 and polymeric vanadia were soluble in HNO_3 and removed from the surface. The state of vanadium in the oxidized catalysts was mainly pentavalent, as shown by XPS, and did not change after acid treatment. Reduction by hydrogen of monolayer vanadia in a 0.2-ML V/TiO_2 catalyst was studied by temperature-programmed reduction (TPR) at different heating rates. A one-site kinetic model is able to account for the TPR data, in spite of the presence of the monomeric and polymeric species. This indicates that these species could be considered equal with respect to the interaction with hydrogen. The activation energy was determined for the catalyst reduction (98 ± 5 kJ/mol). © 2002 Elsevier Science

Key Words: **vanadia/titania catalyst; TPR in hydrogen; FT–Raman spectroscopy; DRIFT; XPS; reduction kinetics modeling; partial oxidation.**

1. INTRODUCTION

V/Ti-oxides are industrially important catalysts used for the partial oxidation of hydrocarbons and the selective reduction of NO_x. They were also studied in some other catalytic reactions such as ammoxidation of alkylaromatics and oxidative dehydrogenation of hydrocarbons. During the last decade *in situ* physical methods have led to progress in the characterization of the surface-active sites of these catalysts. Under dehydrated conditions pure V/Ti-oxides contain isolated monomeric species, polymeric species, and bulk V_2O_5 in amorphous and crystalline states (1–7). In bulk V_2O_5, vanadium is octacoordinated, while in the monomeric and polymeric species, known as "monolayer vanadia," vanadium is tetracoordinated. It is shown (1) that the monolayer vanadia is formed at vanadia loadings, corresponding to the coverage of titania by VO_x species, less than 0.7 theoretical monolayer (ML). One theoretical monolayer is accepted as equal to 1 ML = 10 V-atoms nm^{-2} (4). Monolayer vanadia is found to be more active than bulk V_2O_5 in several reactions (2, 8, 9). However, the reasons for its high catalytic activity and high selectivity toward partial oxidation products are still not clear.

Many reactions of partial oxidation have been shown to proceed via the Mars–van Krevelen mechanism including the steps of reduction of an oxide catalyst by a hydrocarbon and subsequent reoxidation by gaseous oxygen. Often a correlation is observed between the reducibility of vanadia determined by temperature-programmed reduction (TPR) in hydrogen and the catalytic activity. For example, the reducibility of vanadia supported on TiO_2, Al_2O_3, SiO_2 (10) and the activity trend of these catalysts in partial oxidation of methanol (8), ethane (11), toluene, *o*-xylene (12), and oxy-dehydrogenation of propane (13) correlate well between each other.

In spite of the similar coordination of the vanadium atom in the monomeric and polymeric species, their structure differs strongly due to the different length of the V–O bonds. Moreover, contrary to the monomeric species, the polymeric species contain V–O–V oxygen bridges. Hence, different reducibility could be expected in hydrogen, i.e., different pre-exponential factors and/or activation energies. However, the TPR profile of the catalysts containing these two species usually consists of one peak (1). This shows that a differentiation between monomeric and polymeric vanadia by this method is difficult.

It is known that treatment of V/Ti-oxides in aqueous solutions of bases and acids results in partial removal of vanadia from the catalyst surface (2, 4, 14–17). The dissolution of

---

[1] To whom correspondence should be addressed. Fax: 41-21-693 31 90. E-mail: lioubov.kiwi-minsker@epfl.ch.

0021-9517/02 $35.00

bulk V_2O_5 and polymeric species has been reported extensively (2). The surface concentrations of insoluble species has been shown to vary between 0.1 and 0.4 ML (4) or may be higher than 1-ML coverage (16). The insoluble species catalyze oxidative dehydrogenation reactions (4), isopropanol conversion to acetone, and total *o*-xylene oxidation (2). The activity of the catalysts treated in nitric acid (containing only insoluble species) (16) was found to increase in the ammoxidation of methylpyrazine. Hence, the treatment in nitric acid activated the catalyst. However, a decrease in activity after such treatment was reported during *o*-xylene oxidation (2). Therefore, a characterization of the structure of insoluble vanadia is of interest in order to understand the parameters governing catalytic activity/selectivity. Spectroscopic information on the structure of insoluble species is quite limited (4). Recently Besselmann *et al.* (17) found only the monomeric species with tetracoordinated vanadium on the Eurocat V/Ti-oxide catalysts after treatment by NH_4OH by Raman spectroscopy under dehydrated conditions. However, octahedral vanadium coordination followed from the ^{51}V NMR studies of the HNO_3-treated V/Ti-oxide catalyst (16).

The present work is aimed at the study of reducibility of the monomeric and polymeric species in hydrogen by TPR and diffuse reflectance infrared Fourier transform (DRIFT) spectroscopy. Kinetic simulation of the TPR experiments at different heating rates was performed to check whether it was possible to describe the kinetic results using a "one-site" model. The deconvolution of the TPR profiles of supported vanadia catalysts was performed earlier using several Gaussian-shaped curves (10) or multiple-sites models via first-order kinetics (18). To date, the kinetic parameters for the reduction of the vanadia monolayer supported on titania in hydrogen have not previously been determined from TPR experiments. A different solubility of monolayer and bulk vanadia in diluted HNO_3 was used along with XPS and FT–Raman spectroscopy under a controlled atmosphere to investigate the structure of the vanadia species insoluble in nitric acid and the vanadium oxidation state.

2. EXPERIMENTAL

2.1. Catalyst Preparation

A TiO_2 support was prepared by hydrolysis of the tetrapropylorthotitanate (>98%, Fluka). XRD and FT–Raman spectroscopy studies showed that the support possesses an anatase structure. Potassium and sodium were not found in titania as measured by atomic emission spectroscopy (<0.01 wt%). A monolayer catalyst with 1.8 wt% V was prepared via a well-known grafting technique (4, 5) by a three-step $VOCl_3$ vapor deposition on the surface of TiO_2, followed by hydroxylation and drying. An impregnated catalyst containing 11.1 wt% V was synthesized by a three-step wet impregnation with vanadium oxalate solution (synthesized from V_2O_5 (>99.6%, Aldrich) and oxalic acid (>97%, Fluka)). After calcination for 120 min at 723 K the BET surface areas of these catalysts were equal to 57 and 50 $m^2\ g^{-1}$, respectively. The amount of vanadium in the catalysts corresponds to a 0.37- and 2.6-ML coverage of titania by VO_x species (1 ML = 10 V-atoms nm^{-2} (4)). Surface impurities were not found by XPS on these catalysts. Two treatments of the catalysts for 25 min in excess of a 1.2 N aqueous solution of HNO_3 were performed to obtain the samples with insoluble surface vanadia. After washing in deionized water, the catalysts were dried and calcined at 723 K for 30 min in air.

A sample with a smaller coverage by vanadia (0.2 ML) was prepared by wet impregnation of titania with vanadium oxalate solution. The vanadium concentration in this sample was equal to 1.2 wt%, and the BET surface area was 76 $m^2\ g^{-1}$.

2.2. Spectroscopic Methods

Infrared and Raman studies were performed using a FTIR, FT–Raman 2000 spectrometer (Perkin–Elmer). DRIFT or Raman spectroscopy *in situ* cells were attached to a setup described elsewhere (19). The FTIR spectrometer was equipped with a MCT detector, and 0.03 g of the catalyst ground in an agate mortar was placed in a SpectraTech 003-102 DRIFT cell with CaF_2 windows. The DRIFT spectrum of the catalyst reduced in a hydrogen mixture (673 K, 15 vol% H_2/Ar, 30 min) was taken in Ar at 573 K. A single-beam spectrum of the preoxidized catalyst (673 K, 20 vol% O_2/He, 30 min) measured at 573 K was taken as a background. The spectra were obtained by averaging 32 scans with a resolution of 4 cm^{-1}.

A Nd-YAG laser, operating at 1064 nm with a varying power in the range of 10–750 mW, was used in the FT–Raman spectrometer. The Raman *in situ* cell is described elsewhere (7). Sixty-four scans were averaged with a resolution of 4 cm^{-1} to obtain a spectrum. The catalyst in the Raman cell was measured in the flow of dry 20 vol% O_2/Ar mixture (60 ml (STP)/min) at 363 or 523 K after the pretreatment in this mixture at 673 K for 30 min. The conditions of the pretreatment and measurement correspond to the dehydrated conditions (1).

XPS spectra of the catalysts were obtained in an Axis Ultra ESCA system (Kratos, Manchester) with monochromated AlK_α radiation (1486.6 eV) and X-ray power of 150 W. The binding energies scale was referenced against C1s = 285.0 eV line. The $Ti_{2p_{3/2}}$-band maxima were found at the same position (459.0 eV) for both studied samples.

2.3. Temperature-Programmed Reduction

A Micromeritics AutoChem 2910 analyzer with a quartz tubular flow reactor was used for the TPR studies. Hydrogen and other gases were analyzed by a quadrupole mass spectrometer (Thermostar, Pfeiffer Vacuum). The catalysts were pretreated under an oxidative atmosphere (2 vol% O_2, rest He) at 673 K for 30 min and then cooled down in the same mixture to 323 K. After a purge in Ar, the reactor was heated in the flow of ultrahigh purity 4 vol% of H_2 in Ar with a constant heating rate. The measurement was performed at the same flow rate, 20.16 ml (STP)/min. The thermocouple was inserted into the middle of the catalytic bed. The catalyst charge corresponded to the same total surface area of the samples equal to 3.8 m^2. The catalyst grains in the reactor were in the range of 0.35–0.5 mm in order to avoid diffusion limitations.

To study the reduction at four different heating rates, the same catalyst charge of 0.049 g of the fresh 0.2-ML V/TiO_2 catalyst was placed into the reactor. The conversion of hydrogen at the maximum peak temperature (T_{max}) was lower than 25%.

3. RESULTS AND DISCUSSION

The forms in which vanadia is present on the titania surface depend mostly on the vanadia surface concentration, which is generally expressed by titania coverage by VO_x groups. To determine different surface forms of vanadia with respect to their reactivity with hydrogen (TPR), the catalysts with the surface coverage by vanadia of 0.37 and 2.6 ML were mainly investigated before and after the treatment in diluted HNO_3. These catalysts were also examined by FT–Raman spectroscopy under a controlled oxidative atmosphere without water vapor.

3.1. Structure of Surface Vanadia and Vanadium Oxidation State

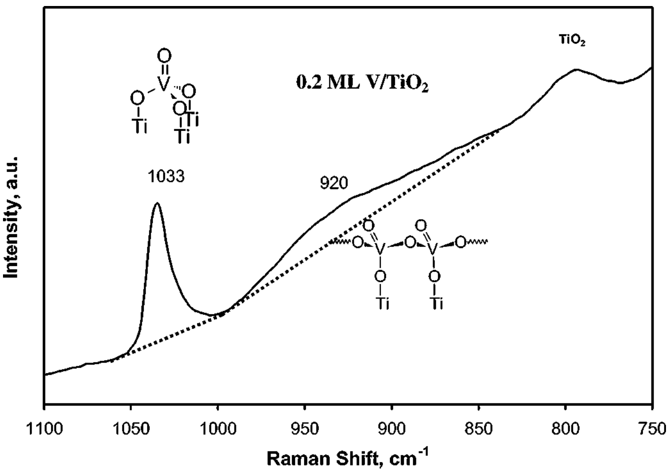

FIG. 1. FT–Raman spectrum of the oxidized 0.2-ML V/TiO_2 catalyst under dehydrated conditions.

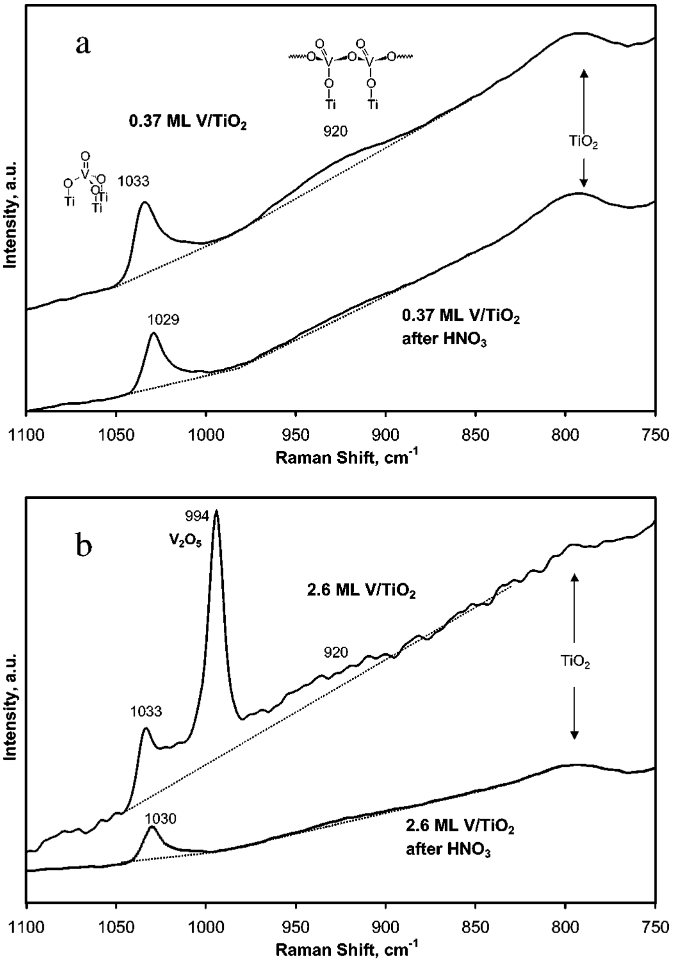

FIG. 2. FT–Raman spectra of the oxidized (a) 0.37- and (b) 2.6-ML V/TiO_2 catalysts under dehydrated conditions before and after treatment in diluted HNO_3.

The FT–Raman spectrum of the 0.2-ML V/TiO_2 catalyst is shown in Fig. 1. The catalyst contains isolated monomeric species (1033 cm^{-1}) and polymeric metavanadate-like species (920 cm^{-1}). In both of these species V^{5+} is tetracoordinated (1).

The FT–Raman spectrum of the 0.37-ML V/TiO_2 catalyst (Fig. 2a) is similar to that of the 0.2-ML V/TiO_2 catalyst (Fig. 1) and contains the monomeric as well as the polymeric species. The increase of the vanadium content from 0.37 to 2.6 ML leads to the appearance of bulk V_2O_5 species with a corresponding band at 994 cm^{-1} (Fig. 2b) together with the monomeric and polymeric species. These spectra are typical for pure V/Ti-oxides under dehydrated conditions (3, 20, 21).

As already mentioned in the Introduction, vanadia supported on titania can be partially removed from the surface by dissolution in aqueous acids and bases (2, 4, 14–17). The reactivity of different vanadia forms with acids depends on the strength of their interaction with the surface of titania. Treatment of the 2.6-ML V/TiO_2 catalyst by diluted HNO_3 leads to the complete disappearance of the bulk V_2O_5 band (Fig. 2b). The monomeric species band intensity

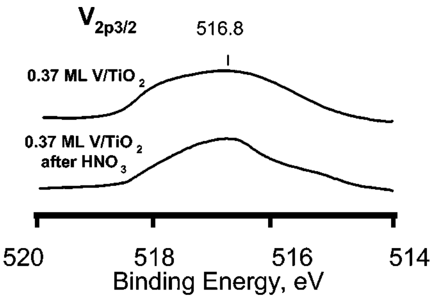

FIG. 3. XPS spectra (smoothed) of the $V_{2p_{3/2}}$region of the oxidized 0.37-ML V/TiO$_2$ catalyst before and after treatment in diluted HNO$_3$.

almost does not change. A drastic decrease of the polymeric species band (if not a complete removal) is observed in the spectra of both catalysts (Fig. 2). The possible presence of the polymeric species after acid treatment and calcination at 723 K could be a result of dehydration of the retained hydrated monomeric species at elevated temperature (22).

Additionally, it is observed that the V=O band for the monomeric species shifts 3–4 cm^{-1} to lower wavenumbers after the acid treatment. This shift corresponds to a negligible increase of the V=O interatomic distance (less than 0.002 Å (23)) and is due to the decrease of vanadia concentration (24). The accompanied increase of the Ti–OH group concentration (discussed later) probably provides increased hydrogen bonding with oxygen of the vanadyl groups and explains the lengthening of the V=O bond. Similar effects were found during direct water vapor treatment of vanadia catalysts (1, 20).

XPS measurements of the 0.37-ML V/TiO$_2$ catalyst before and after treatment in HNO$_3$ and calcination at 723 K were also performed. The $V_{2p_{3/2}}$ signals were noisy because of the small concentration of vanadium in the studied catalysts. This explains the asymmetric shape of the observed peaks, but it is clearly seen (Fig. 3) that the main oxidation state of vanadium is similar in both samples (516.8 eV) and corresponds to that of V^{5+} (25). The V/(Ti + V) atomic surface ratio was observed to decrease after the treatment, but was not quantified due to the high experimental error.

Hence, the polymeric and V$_2$O$_5$ species are removed during the acid treatment. Vanadium in all species found in the catalysts after the treatment is pentavalent and tetracoordinated contrary to the results (16), where only octacoordinated vanadium was determined by ^{51}V NMR. The difference may be due to a much higher concentration of insoluble species, in the latter case explained by the presence of impurities in the catalyst as well as due to spectroscopic measurements under ambient conditions in the presence of water vapor.

3.2. *Reducibility of Surface Vanadia Species by Hydrogen*

TPR profiles of the same catalysts before and after the HNO$_3$ treatment are shown in Figs. 4a and 4b. It is seen that the amount of hydrogen consumed for the treated catalysts decreased two and seven times, respectively, for the 0.37- and 2.6-ML V/TiO$_2$ catalysts. This indicates that vanadia is partially removed in HNO$_3$ in accordance with the FT–Raman spectra (Fig. 2). The surface vanadia concentration corresponds to the values reported by Grzybowska-Swierkosz (4) in the range of 0.1–0.4 ML.

Another important observation is that $T_{\max}$ for the reduction of the catalysts after the acid treatment shifts to lower temperatures (770–780 K) independently of the initial coverage by vanadia (0.37 or 2.6 ML). According to the FT–Raman spectroscopy data the main species retained on the surface is the monomeric species (Fig. 2). Hence, $T_{\max}$ for the reduction of this species must be equal to 770–780 K or be slightly lower. The latter suggests the existence of some amount of the polymeric species reducible at a higher temperature than the monomeric species.

The difference TPR profile corresponding to the removal of mainly V$_2$O$_5$ from the 2.6-ML V/TiO$_2$ catalyst has a maximum at 852 K (Fig. 4b). Bulk crystalline V$_2$O$_5$ can be reduced only at much higher temperature (>950 K) (5, 6, 26).

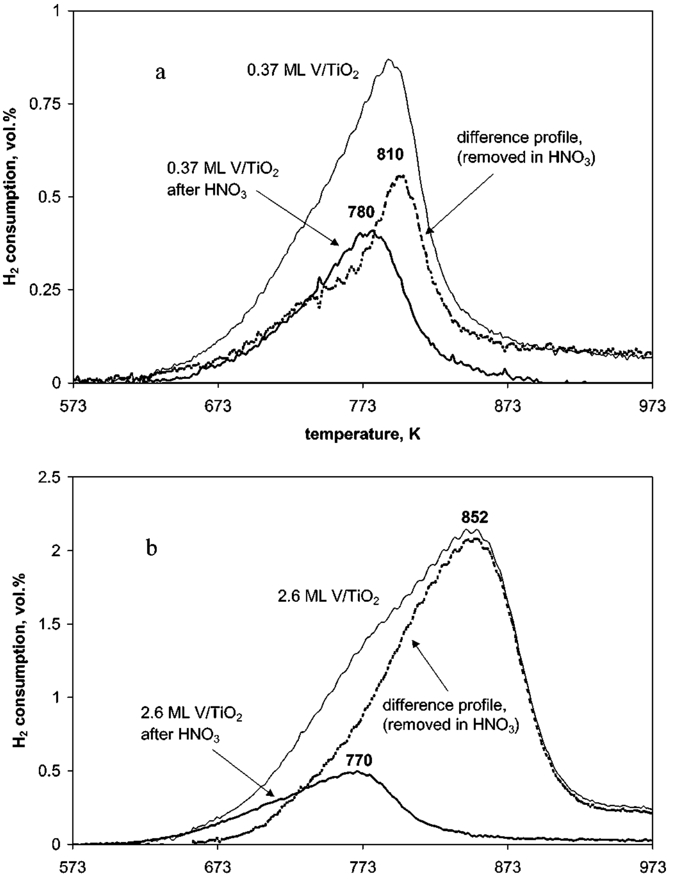

FIG. 4. TPR profiles of the (a) 0.37- and (b) 2.6-ML V/TiO$_2$ catalysts before and after treatment in HNO$_3$. Total flow rate of the 4 vol% H$_2$/Ar mixture: 20.16 ml (STP)/min, heating rate 20 K/min.

Hence, the peak with a maximum at 852 K was assigned to the reduction of amorphous V_2O_5. The difference between bulk crystalline and amorphous V_2O_5 consists of the fact that the latter is present in the form of nanocrystalline particles and/or thin layers. The maximum of difference profile for the 0.37-ML V/TiO_2 catalyst is also shifted to higher temperatures (810 K) with respect to T_{max} for the reduction of the monomeric species ($\leq$770–780 K) (Fig. 4a). T_{max} at 810 K is assigned to the reduction of the polymeric species as the acid treatment of the 0.37-ML V/TiO_2 catalyst removes mainly the polymeric species (Fig. 2a).

Due to the HNO_3 treatment, it was possible to estimate the T_{max} of the monomeric species reduction. The monomeric species seems to be easily reducible in hydrogen. T_{max} for the reduction of the polymeric species is slightly higher (30–40 K). The reduction of amorphous bulk V_2O_5 takes place at about 70–80 K higher than that observed in the case of the monomeric species. Thus with an increase coverage of titania by vanadia and vanadia polymerization degree, the TPR peak should shift to higher temperatures in accordance with the literature data (27–29). This trend, however, cannot be extended to vanadia on other supports because of the change in the vanadia–support interaction dependent on the electronegativity of the support cation (8, 11). Contrary to the reduction of vanadia/titania catalysts Stobbe-Kreemers *et al.* (30) found a decrease of T_{max} with increased vanadia loading on alumina, which was assigned to an easier reduction of the polymeric compared to the monomeric species. Hence, the nature of the support affects the reducibility of the vanadia species mainly via the V–O–Me (Me = Ti, Al, Mg, etc.) bonds (8, 10, 11, 13).

3.3. Kinetics and Modeling of the Reduction of Monolayer Vanadia by Hydrogen

In order to determine the energy of activation of the reduction of only the monolayer vanadia, the 0.2-ML V/TiO_2 catalyst which does not contain any V_2O_5 species (Fig. 1) was reduced in hydrogen at different heating rates. The experimental TPR curves are shown in Fig. 5. The increase of the heating rate from 4.99 to 63.7 K/min results in a shift of T_{max} to higher values by more than 100 K. The activation energy for the reduction can be estimated by (31)

$$\ln(\beta/T_{max}{}^2) = -E_a/(8.314\ T_{max}) + \text{const}, \qquad [1]$$

where β is the heating rate (K/min), E_a is the activation energy of reduction (J/mol), and 8.314 is the universal gas constant (J/(mol K)). The E_a value was estimated equal to 98 ± 5 kJ/mol (Fig. 6).

As the conversion of hydrogen was relatively low, the equation for the mass balance of hydrogen in a gradientless reactor can be used; for example,

$$\Delta y Q_n = -RmZ_0, \qquad [2]$$

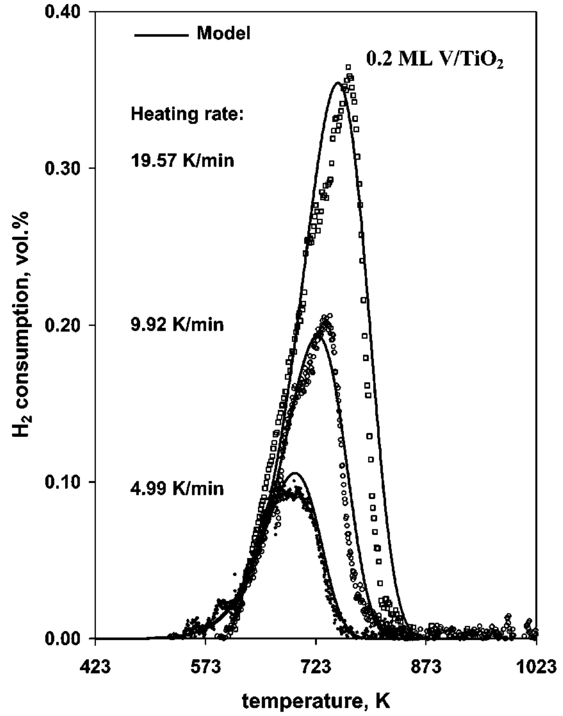

FIG. 5. TPR profiles of the 0.2-ML V/TiO_2 catalyst at different heating rates (points, experiments; curves, simulation using a one-site model). Total flow rate of the 4 vol% H_2/Ar mixture is 20.16 ml (STP)/min.

where Δy is the molar fraction of the consumed hydrogen (difference between the molar fraction of hydrogen at the reactor inlet and reactor outlet), Q_n is the total molar flow (mol/s), m is the mass of the catalyst (kg), R is the rate of hydrogen consumption related to the moles of reducible sites (1/s), and Z_0 is the total concentration of reducible sites in the catalyst (mol/kg).

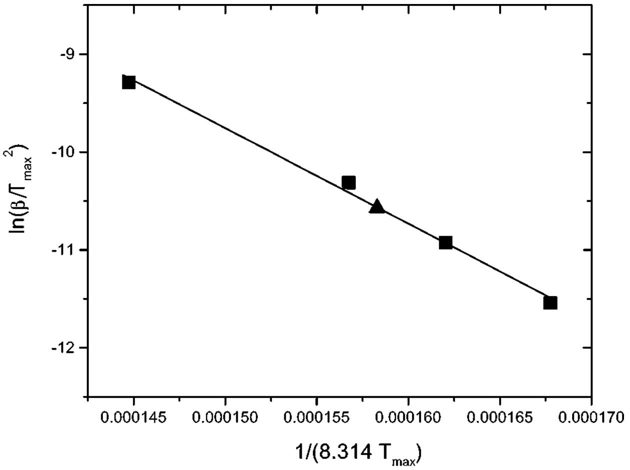

FIG. 6. Determination of activation energy for the reduction of the 0.2-ML V/TiO_2 catalyst in hydrogen at different heating rates (squares, total flow rate 20.16 ml (STP)/min, triangles, 10.19 ml (STP)/min).

During the reduction of the 0.2- and 0.37-ML V/TiO_2 catalysts the O/V atomic ratio was found to be 1.6 O-atom to 1 V-atom. For the 2.6-ML V/TiO_2 catalyst containing bulk vanadia this ratio was found to be lower (0.95). The literature O/V ratios were reported in the range of 1–1.53. They were equal to 1 (32), 1.1–1.2 (3), 1.5 (33), and 1.53 (10). The values higher than 1 were explained by the partial transformation of V^{5+}-containing vanadia into the V^{2+}-containing species (33). Another explanation is that some part of hydrogen may be retained on the surface in the form of hydroxyl groups attached to the reduced vanadia species as proposed by Haber *et al.* (32) and Went *et al.* (3). Both assumptions need further experimental confirmation.

The processes of reduction of the monolayer vanadia species on the titania support are not complicated by subsurface–surface diffusion as in the case of the reduction of bulk crystalline V_2O_5 (26). Thus the rate equation of the surface vanadia reduction was assumed to be first order in hydrogen pressure and in coverage by reducible species ($\theta = Z/Z_0$); for example,

$$R = d\theta/dt = k_0 p\theta \exp(-E_a/(8.314\,T)), \qquad [3]$$

where k_0 is a preexponentional factor (1/(Pa s)), t is the time (s), T is the temperature as a function on time ($T = 323 + \beta t$) (K), Z is the concentration of reducible sites at any time (mol/kg), and p is the partial pressure of hydrogen (Pa).

The simulation of the TPR curves at different heating rates was performed using Berkeley Madonna software (Berkeley, CA). The found value of $E_a = 97.6$ kJ/mol (Fig. 6) was used, and only the value of the preexponentional factor was varied. It was estimated to be equal to 4.0 $Pa^{-1} \cdot s^{-1}$. It is seen from Fig. 5 that the simulated TPR peaks width at half-height and the amount of the consumed hydrogen, as seen by the area under the curve, correspond well to the experimental data. The shapes of the simulated and experimental curves turned out to be slightly different. Experimental curves were less symmetric and characterized by a steep decrease in temperature after the maximum. The presence of different reducible sites on the catalyst surface could explain the latter fact. However, the application of a "two-sites" model did not significantly improve the simulation to fit to the experimental data.

3.4. DRIFT Study of the Surface Oxygen Involved in the Vanadia Reduction by Hydrogen

To determine what happens with surface vanadia species and hydroxyl groups during the reduction in hydrogen, a DRIFT study was performed, and the spectrum was related to the spectrum of the catalyst in the oxidized state.

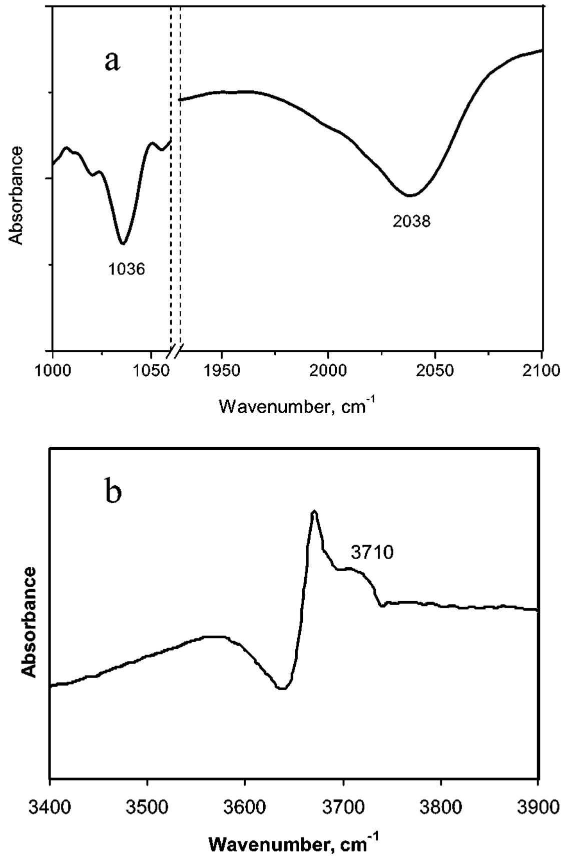

FIG. 7. DRIFT spectra of the vanadia (a) and hydroxyl (b) regions of the 0.37-ML V/TiO_2 catalyst after the reduction in the 15 vol% H_2/Ar mixture at 673 K for 30 min. The measurement was performed in Ar at 573 K. The spectrum of the oxidized catalyst is taken as a background.

The negative absorbance bands at 1036 and 2038 cm^{-1} observed in the DRIFT spectrum of the 0.37-ML V/TiO_2 catalyst (Fig. 7a) after 30 min of reduction at 673 K correspond to the V=O stretching band and its first overtone in the monomeric species, respectively (34–36). The negative bands indicate the reduction of the monomeric species under these relatively mild conditions. No new vanadia bands appear in the region of interest after the reduction. The region below 950 cm^{-1}, characteristic for the polymeric species, could not be studied because of a strong absorbance by the titania support.

The hydroxyl group region in the DRIFT spectrum shown in Fig. 7b possesses negative (~3650 cm^{-1}) as well as positive features (~3670 and 3710 cm^{-1}). The total picture implies the shift of the hydroxyl region to the higher wavenumbers. This is indicative of hydroxyl groups more basic on the reduced catalyst if compared to the oxidized catalyst. Dines *et al.* (37), after hydrogen reduction of the vanadia/titania catalyst, found the disappearance of the Brønsted sites by ammonia and pyridine adsorption. The positive bands at 3670 and 3710 cm^{-1} indicate the appearance of new hydroxyl groups or an increase of their concentration after the reduction. These two bands are observed in the spectrum of a pure titania–anatase used as a support (35, 38).

Topsoe *et al.* (35) assigned the 3650-cm^{-1} band to the hydroxyl groups attached to vanadia sites. Upon the reduction the disappearance of this band and the appearance of the 3670- and 3715-cm^{-1} bands assigned to the hydroxyl groups of titania are reported. This is explained by the agglomeration of vanadia species during reduction and a liberation of some titania sites involved in the formation of the monomeric vanadia species. A similar mechanism was proposed earlier for the vanadia/alumina catalyst by Sobalik *et al.* (39). Recently, using *in situ* XAFS experiments, Ruitenbeek *et al.* (40) demonstrated the possibility of V^{3+} formed upon reduction not to agglomerate but to migrate into the bulk of the alumina support. This process was reversible, as the isolated monomeric species were formed again upon reoxidation. The present study shows evidence for the disappearance of V=O groups upon the reduction by hydrogen and the formation of Ti–OH groups. However, the nature of hydroxyl groups associated with supported vanadia species and the structure of reduced vanadia species need further clarification.

4. CONCLUSIONS

Three types of vanadia species were determined on vanadia/titania catalysts consisting of 0.2–2.6 ML of VO_x on the titania surface. Their reducibility in hydrogen was characterized by the peak maximum in the TPR profiles indicating isolated monomeric species: ($\leq$ 770–780 K), polymeric species (810 K), and bulk amorphous V_2O_5 (852 K). The monomeric species was the easiest to reduce.

During the reduction, the V=O bond of the monomeric species with tetracoordinated vanadium was observed to disappear, as shown by DRIFT spectroscopy. A formation of new hydroxyl groups with a basic character probably associated with titania was observed.

A “one-site” kinetic model describes accurately the TPR profiles obtained during the reduction of the 0.2-ML V/TiO_2 catalyst in hydrogen, containing the monomeric and polymeric vanadia. This indicates that these species could be considered equal with respect to the interaction with hydrogen. An activation energy of 98 ± 5 kJ/mol was obtained for the reduction of monolayer vanadia.

Bulk amorphous V_2O_5 and polymeric vanadia were soluble in nitric acid and removed by acid from the surface. The monomeric species was the most stable in diluted HNO_3 suggesting strong attachment to the titania support.

The state of vanadium in the preoxidized catalysts was mainly pentavalent, as shown by XPS, and did not change after acid treatment.

ACKNOWLEDGMENTS

The authors thank the Swiss National Science Foundation for financial support. XPS measurements by N. Xanthopoulos (DM-EPFL) and useful discussions with Dr. B. Monnerat (LGRC-EPFL) are gratefully acknowledged.

REFERENCES

1. Wachs, I. E., and Weckhuysen, B. M., *Appl. Catal. A Gen.* **157**, 67 (1997).
2. Bond, G. C., and Vedrine, J. C., *Catal. Today* **20**, 171 (1994).
3. Went, G. T., Leu, L.-J., and Bell, A. T., *J. Catal.* **134**, 479 (1992).
4. Grzybowska-Swierkosz, B., *Appl. Catal. A Gen.* **157**, 263 (1997).
5. Bond, G. C., *Appl. Catal. A Gen.* **157**, 91 (1997).
6. Bulushev, D. A., Rainone, F., Kiwi-Minsker, L., and Renken, A., *Langmuir* **17**, 5276 (2001).
7. Bulushev, D. A., Kiwi-Minsker, L., Zaikovskii, V. I., and Renken, A., *J. Catal.* **193**, 145 (2000).
8. Deo, G., and Wachs, I. E., *J. Catal.* **146**, 323 (1994).
9. Courcot, D., Grzybowska, B., Barbaux, Y., Rigole, M., Ponchel, A., and Guelton, M., *J. Chem. Soc., Faraday Trans.* **92**, 1609 (1996).
10. Arena, F., Frusteri, F., and Parmaliana, A., *Appl. Catal. A Gen.* **176**, 189 (1999).
11. Banares, M. A., Martinez-Huerta, M. V., Gao, X., Fierro, J. L. G., and Wachs, I. E., *Catal. Today* **61**, 295 (2000).
12. van Hengstum, A. J., van Ommen, J. G., Bosch, H., and Gellings, P. J., *Appl. Catal.* **8**, 369 (1983).
13. Lemonidou, A. A., Nalbandian, L., and Vasalos, I. A., *Catal. Today* **61**, 333 (2000).
14. Centi, G., Giamello, E., Pinelli, D., and Trifiro, F., *J. Catal.* **130**, 220 (1991).
15. Nogier, J. P., *Catal. Today* **20**, 23 (1994).
16. Bondareva, V. M., Andrushkevich, T. V., and Lapina, O. B., *Catal. Today* **61**, 173 (2000).
17. Besselmann, S., Loffler, E., and Muhler, M., *J. Mol. Catal. A Chem.* **162**, 401 (2000).
18. Koranne, M. M., Goodwin, J. G., and Marcelin, G., *J. Catal.* **148**, 369 (1994).
19. Bulushev, D. A., Kiwi-Minsker, L., and Renken, A., *Catal. Today* **57**, 231 (2000).
20. Jehng, J.-M., Deo, G., Weckhuysen, B. M., and Wachs, I. E., *J. Mol. Catal. A Chem.* **110**, 41 (1996).
21. Olthof, B., Khodakov, A., Bell, A. T., and Iglesia, E., *J. Phys. Chem. B* **104**, 1516 (2000).
22. Balzhinimaev, B. S., and Pinaeva, L. G., *Kinet. Catal.* **36**, 52 (1995).
23. Hardcastle, F. D., and Wachs, I. E., *J. Phys. Chem.* **95**, 5031 (1991).
24. Wachs, I. E., *Catal. Today* **27**, 437 (1996).
25. Nogier, J. P., and Delamar, M., *Catal. Today* **20**, 109 (1994).
26. Bosch, H., Kip, B. J., van Ommen, J. G., and Gellings, P. J., *J. Chem. Soc., Faraday Trans. I* **80**, 2479 (1984).
27. Matralis, H. K., Papadopoulou, C., Kordulis, C., Elguezabal, A. A., and Corberan, V. C., *Appl. Catal. A Gen.* **126**, 365 (1995).
28. Baiker, A., Dollenmeier, P., Glinski, M., and Reller, A., *Appl. Catal.* **35**, 351 (1987).
29. Bond, G., and Tahir, S. F., *Appl. Catal.* **71**, 1 (1991).
30. Stobbe-Kreemers, A. W., van Leerdam, G. C., Jacobs, J.-P., Brongersma, H. H., and Scholten, J. J. F., *J. Catal.* **152**, 130 (1995).
31. Hurst, N. W., Gentry, S. J., Jones, A., and McNicol, B. D., *Catal. Rev.—Sci. Eng.* **24**, 233 (1982).
32. Haber, J., Kozlowska, A., and Kozlowski, R., *J. Catal.* **102**, 52 (1986).

33. Malet, P., Munoz-Paez, A., Martin, C., and Rives, V., *J. Catal.* **134**, 47 (1992).
34. Busca, G., Centi, G., Marchetti, L., and Trifiro, F., *Langmuir* **2**, 568 (1986).
35. Topsoe, N.-Y., Topsoe, H., and Dumesic, J. A., *J. Catal.* **151**, 226 (1995).
36. Scharf, U., Schneider, M., Baiker, A., and Wokaun, A., *J. Catal.* **149**, 344 (1994).
37. Dines, T. J., Rochester, C. H., and Ward, A. M., *J. Chem. Soc., Faraday Trans.* **87**, 1611 (1991).
38. Primet, M., Pichat, P., and Mathieu, M. V., *J. Phys. Chem.* **75**, 1216 (1971).
39. Sobalik, Z., Kozlowski, R., and Haber, J., *J. Catal.* **127**, 665 (1991).
40. Ruitenbeek, M., van Dillen, A. J., de Groot, F. M. F., Wachs, I. E., Geus, J. W., and Koningsberger, D. C., *Topics Catal.* **10**, 241 (2000).